

Unexpected entrance-channel effect in the fission of $^{216}\text{Ra}^*$

A. Yu. Chizhov, M. G. Itkis, I. M. Itkis, G. N. Kniajeva, E. M. Kozulin, N. A. Kondratiev, I. V. Pokrovsky,*
R. N. Sagaidak,† V. M. Voskressensky, and A. V. Yerein

Flerov Laboratory of Nuclear Reactions, Joint Institute for Nuclear Research, RU-141980 Dubna, Moscow region, Russia

L. Corradi, A. Gadea, A. Latina, A. M. Stefanini, S. Szilner, M. Trotta, and A. M. Vinodkumar
Istituto Nazionale di Fisica Nucleare, Laboratori Nazionali di Legnaro, Via Romea 4, I-35020 Legnaro, Padova, Italy

S. Beghini, G. Montagnoli, and F. Scarlassara
Dipartimento di Fisica, Università di Padova, Via Marzolo 8, I-35131 Padova, Italy

A. Ya. Rusanov
Institute of Nuclear Physics of the National Nuclear Center of Kazakhstan, 480082 Almaty, Kazakhstan

F. Hanappe
Université Libre de Bruxelles, PNTPM, CP229, Avenue F.D. Roosevelt, B1050 Brussels, Belgium

O. Dorvaux, N. Rowley, and L. Stuttgé
IReS, UMR7500, IN2P3-CNRS/Université Louis Pasteur, BP28, F-67037, Strasbourg Cedex 2, France
(Received 19 July 2002; published 31 January 2003)

We have studied the mass and energy distributions of fission fragments from the two reactions $^{12}\text{C} + ^{204}\text{Pb}$ and $^{48}\text{Ca} + ^{168}\text{Er}$ that lead to the same compound nucleus $^{216}\text{Ra}^*$. Despite the fact that the excitation energy was around 40 MeV in both cases, the contribution from asymmetric fission in the first reaction is only around 1.5% but is about 30% in the second. This marked increase in the yield of asymmetric products is connected to the quasifission process, in which important shell effects become evident. The mass-energy distributions are interpreted in terms of an independent decay mode competing with the normal fusion-fission process and possibly leading to a significant suppression of the fusion cross section itself.

DOI: 10.1103/PhysRevC.67.011603

PACS number(s): 25.70.Gh, 24.75.+i, 25.70.Jj, 27.80.+w

The multimodal nature of the mass-energy distributions (MEDs) of fission fragments from both the low-energy and spontaneous fission of heavy nuclei is now widely recognized [1–4]. Our recent efforts have been concentrated on investigations of multimodal structures in the region of transitional nuclei, $219 \leq A_{\text{CN}} \leq 226$, which has so far been poorly studied. We have previously investigated these properties for $^{220}\text{Ra}^*$ [5], $^{219}\text{Ac}^*$, and $^{220,224,226}\text{Th}^*$ [6,7]; in the present work we report on the MED of fission fragments from $^{216}\text{Ra}^*$. In contrast to our previous experiments, the compound nucleus was populated through two different projectile-target combinations, namely $^{12}\text{C} + ^{204}\text{Pb}$ and $^{48}\text{Ca} + ^{168}\text{Er}$. The results turn out to be rather unexpected.

The experiments were carried out using ion beams from the XTU Tandem+ALPI accelerator complex of the Laboratori Nazionali di Legnaro. The beam energy range was $E_{\text{lab}} = 56\text{--}90$ MeV in the case of ^{12}C (intensity 5–10 pA) and 180–208 MeV in the case of ^{48}Ca (1–5 pA). In this paper we present results of measurements only at the beam energies $E_{\text{lab}} = 73$ MeV for ^{12}C and 194 MeV for ^{48}Ca . These lead to approximately the same excitation energy in the compound nucleus $^{216}\text{Ra}^*$ ($E_{\text{CN}}^* = 40.4$ and 39.6 MeV, respectively, using empirical masses from Ref. [8]). Reaction prod-

ucts were detected by the two-arm time-of-flight spectrometer CORSET [5,7,9], each arm of which consisted of a compact start detector and of an x, y position-sensitive stop detector, 6×4 cm in size, both based on microchannel plates. In both reactions the arms of the spectrometer were positioned so that the center-of-mass angle between detected fragments was around 180° . The shortest flight path was 14 cm. The mass resolution of the spectrometer was estimated to be 3–5 u [5,9]. Targets of highly enriched isotopes ^{204}Pb and ^{168}Er about $170 \mu\text{g}/\text{cm}^2$ in thickness were used, both formed by evaporation of the metal onto $15\text{--}20 \mu\text{g}/\text{cm}^2$ carbon backings.

The data processing assumed standard two-body kinematics as presented in Refs. [9,10]. Fragment energy losses in the target, the backing and the start detectors were taken into account. Special attention was paid to angular folding correlations both in and out of the reaction plane, and only events corresponding to a two-body process with full linear momentum transfer were considered.

Figure 1 displays the main characteristics of the fission fragment MED for both reactions. Figure 1(a) shows the two-dimensional matrix of counts $N(M, \text{TKE})$ as a function of mass and total kinetic energy for the $^{12}\text{C} + ^{204}\text{Pb}$ reaction. Figure 1(b) shows the corresponding fission-fragment mass distribution (MD). The characteristic triangular shape of the matrix and the Gaussian form of the integrated MD indicate that the influence of shell effects is small for this system. It is

*Electronic address: pokrovsk@cv.jinr.ru

†Electronic address: sagaidak@sunvas.jinr.ru

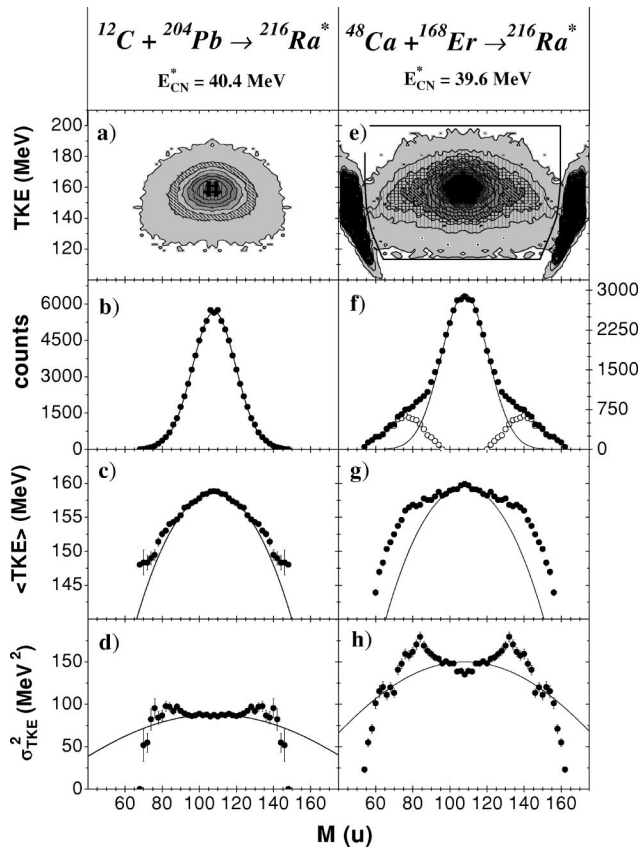


FIG. 1. MED of the correlated fission fragments from the reactions $^{12}\text{C} + ^{204}\text{Pb} \rightarrow ^{216}\text{Ra}^*$ (left panels) and $^{48}\text{Ca} + ^{168}\text{Er} \rightarrow ^{216}\text{Ra}^*$ (right panels) as a function of fragment mass M : (a) and (e) show the two-dimensional matrices $N(M, \text{TKE})$; (b) and (f) show the integrated mass distributions. Solid curves are Gaussian fits to the symmetric (central) components and open circles (right-hand panel only) correspond to the extracted asymmetric contribution; (c) and (g) show $\langle \text{TKE} \rangle$. Solid curves represent the parabolic approximation to the symmetric component [7]; (d) and (h) show the variances σ_{TKE}^2 . Solid curves describe the symmetric components assuming a constant value of $\langle \text{TKE} \rangle^2(M) / \sigma_{\text{TKE}}^2(M)$ [7].

precisely this type of MD which is predicted by the liquid-drop [11] and diffusion models [12] in the case of a relatively hot nucleus. The average total kinetic energy and its variance σ_{TKE}^2 are shown in Figs. 1(c) and 1(d) as functions of the fission-fragment mass. The $\langle \text{TKE} \rangle$ for the heavy (and complementary light) fragment masses, starting from $M \approx 128$, becomes wider than the parabola that describes the symmetric (central) part of the spectrum [Fig. 1(c)]. The function σ_{TKE}^2 possesses small peaks in the asymmetric mass regions. Since the energy characteristics of fission fragments are sensitive to the presence of an asymmetric fission mode [1,4,5,7], the observed irregularities point to a small asymmetric contribution estimated at around 1.5%. This is what one would predict from the systematics of asymmetric yields as a function of nucleon composition [1,5]. Thus in the $^{12}\text{C} + ^{204}\text{Pb}$ reaction, we observe a clear picture of the $^{216}\text{Ra}^*$ fusion-fission (FF), in agreement with our expectations.

The fission of this nucleus has also been investigated [13] using the giant dipole resonance at excitation energies near

to the fission barrier ($E_{\text{CN}}^* \approx 11-15$ MeV). As in our observations, no significant contribution from asymmetric fission was seen.

The right panels of Fig. 1 show the same quantities for the $^{48}\text{Ca} + ^{168}\text{Er}$ reaction. All the distributions differ significantly from those observed for $^{12}\text{C} + ^{204}\text{Pb}$. In the $N(M, \text{TKE})$ matrix of Fig. 1(e) the reaction products having masses close to those of the projectile and target are identified as quasi-elastic and deep-inelastic events, and we will not consider them. Reaction products in the mass range $\approx 55-160$ can be identified as totally relaxed events, i.e., as fission fragments. We have outlined them in Fig. 1(e). Henceforth we consider the properties of only these events. Their mass distributions are shown in Fig. 1(f). The large contribution ($\sim 30\%$) of the asymmetric fission mode is immediately evident, manifesting itself in the form of wide “shoulders.” The symmetric fission component is described by a Gaussian shape wider than that for the ^{12}C reaction ($\sigma_M^2 = 156$ and 132 u², respectively). This increase in variance is consistent with the results of Ref. [14], where it is shown that σ_M^2 increases approximately linearly with $\langle I^2 \rangle$. According to Ref. [15], the critical angular momentum is $31\hbar$ for the $^{12}\text{C} + ^{204}\text{Pb}$ reaction and $54\hbar$ for $^{48}\text{Ca} + ^{168}\text{Er}$. Thus the observed increase of σ_M^2 agrees with the expectations for normal symmetric fission of the excited CN. The shape of the curve obtained for $\langle \text{TKE} \rangle$ [Fig. 1(g)] is far from parabolic, and is much wider than the parabola of Fig. 1(c). As for σ_{TKE}^2 , the peaks in the mass regions 80–90 and 130–140 are more pronounced. Thus in the ^{48}Ca reaction we observe a strong increase (by a factor of ~ 20) in the contribution of asymmetric fission compared with the ^{12}C reaction. This increase is also reflected in the energy distributions of the fragments. It is interesting to note that this effect is observed at all energies around the fusion barrier in the ^{48}Ca reaction (these other energies are not considered in detail in the present paper), though its importance decreases sharply with increasing excitation energy.

In the framework of normal fission, proceeding through the formation of a CN, it is difficult to understand our observations since it is well known that increasing the angular momentum decreases the influence of shell effects [16]. In the case of a massive projectile such as ^{48}Ca , as opposed to the ^{12}C reaction, the most plausible explanation is a large contribution from quasifission (QF), a process bypassing the usual CN stage. This conclusion is supported by the results of previous works [17,18], where for $^{58}\text{Ni} + ^{165}\text{Ho}$ [17], $^{48}\text{Ti} + ^{166}\text{Er}$ and $^{60}\text{Ni} + ^{154}\text{Sm}$ [18] it was found that there is a clear asymmetry in the backward and forward directions for different mass regions. This points to the nonequilibrium nature of the process, i.e., to QF. Indeed a decomposition of the integrated mass yields into compound nucleus and QF components was performed in the above papers.

In the present case, the processes of normal fusion-fission (the symmetric component in the yield) and quasifission (the asymmetric one) compete with each other, and we observe the combined effect of these two independent reaction channels. The quasifission mass distribution, obtained as the difference between the experimental yield and the (Gaussian) fusion-fission yield,

$$Y_{\text{QF}} = Y_{\text{exp}} - Y_{\text{FF}}, \quad (1)$$

is shown by the open symbols in Fig. 1(f). As seen in Fig. 1(f), the QF mass distribution has two bumps and, surprisingly, its shape is very reminiscent of the standard picture of mass yields for the low-energy fission of actinide nuclei (though slightly wider), since the average mass of the heavy fragment is around 140. It is well known that in the usual low-energy fission of heavy nuclei two principal modes—symmetric (s) and asymmetric (a)—are obtained with different yields Y_i and different energy characteristics TKE_i and $\sigma_{\text{TKE},i}^2$ (with $i=s$ or a). In the present case one can again talk of the two independent modes QF and FF. Thus, although there is a formal analogy with low-energy fission, the modes are different, and their nature is very different too. Following this argument, we must conclude that in the region where the FF and QF modes overlap, the observed fission fragments may have the same mass, as well as the same TKE, but may be born in these two very different processes. Thus the standard procedure of decomposing the MED [1] can be applied. In addition to Eq. (1) we have

$$\text{TKE}_{\text{expt}} = \text{TKE}_{\text{FF}}(Y_{\text{FF}}/Y_{\text{expt}}) + \text{TKE}_{\text{QF}}(Y_{\text{QF}}/Y_{\text{expt}}), \quad (2)$$

$$(\sigma_{\text{TKE}}^2)_{\text{expt}} = (\sigma_{\text{TKE}}^2)_{\text{FF}}(Y_{\text{FF}}/Y_{\text{expt}}) + (\sigma_{\text{TKE}}^2)_{\text{QF}}(Y_{\text{QF}}/Y_{\text{expt}}) + (\text{TKE}_{\text{FF}} - \text{TKE}_{\text{QF}})^2(Y_{\text{FF}}Y_{\text{QF}}/Y_{\text{expt}}^2), \quad (3)$$

where all these quantities are considered as functions of M . The maximum in σ_{TKE}^2 is achieved for $Y_{\text{FF}} \approx Y_{\text{QF}}$. It can be seen from Fig. 1(f) that for the heavy fragments the extracted quasi-fission component has a yield equal to that for FF near $M_{\text{H}} = 132$, i.e., exactly where the experimental variance is largest. Thus our assumption on the superposition of two independently formed modes appears well justified, and we can decompose the experimental distributions into two components.

Figure 2 shows the results of such a decomposition for $^{12}\text{C} + ^{204}\text{Pb}$ (left panels) and for $^{48}\text{Ca} + ^{168}\text{Er}$ (right panels). The solid curves show the characteristics of the symmetric component (as in Fig. 1) and the filled circles show the extracted asymmetric component. For $^{12}\text{C} + ^{204}\text{Pb}$ one has classic asymmetric fusion-fission whereas for $^{48}\text{Ca} + ^{168}\text{Er}$ one has an overwhelming contribution to the asymmetric component from QF, whose characteristics differ from those of the FF process. In particular the yield of the QF component has a much broader mass distribution and the corresponding σ_{TKE}^2 is significantly larger. The detailed shapes of the two energy curves also clearly differ.

A hypothesis explaining the main properties of the QF process is the influence of relatively strong shell effects. The arrows in Fig. 2(d) show the positions of the spherical closed shells with $Z=28$, and 50 and $N=50$, and 82 and their complementary masses, derived from the simple assumption of charge/mass equilibration. The major part of the QF component fits into the region of these shells, and the maximum of Y_{QF} is a “compromise” between $Z=28$, $N=50$, and $N=82$. Thus, it is clear that the shell structure of the fragments formed in the mass ranges $M_{\text{L}} = 65-68$ and $M_{\text{H}} = 130-150$

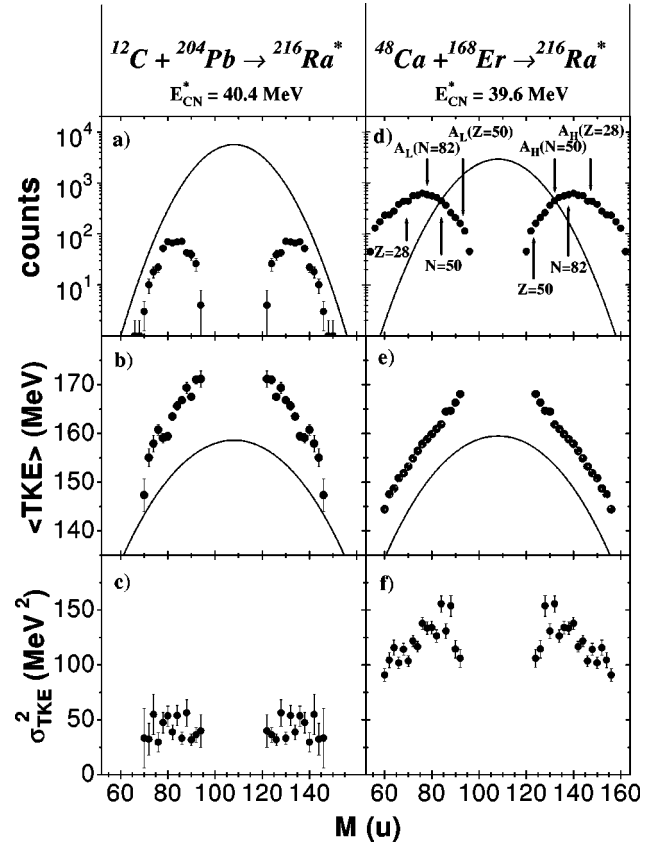


FIG. 2. MED for the extracted asymmetric components from the reactions $^{12}\text{C} + ^{204}\text{Pb}$ (left panels) and $^{48}\text{Ca} + ^{168}\text{Er}$ (right panels) as a function of fragment mass M : (a) and (d) show integrated mass distributions. Solid curves are Gaussian fits to the symmetric component (as in Fig. 1); (b) and (e) show $\langle \text{TKE} \rangle$. Solid curves are the parabolic approximations to the symmetric components (as in Fig. 1); (c) and (f) show the variances σ_{TKE}^2 . For the $^{48}\text{Ca} + ^{168}\text{Er}$ reaction the lower arrows denote masses corresponding to closed spherical shells and the upper arrows denote the masses of the complementary fragments (see text).

strongly favors the QF process, the shells in both the light and heavy fragments playing an important role.

The manifestation of shell effects in the QF process has been discussed in a number of experimental and theoretical papers [19–25]. However, these have generally considered cases in which heavy projectiles (U ions in reactions with inverse kinematics) interact with actinide targets. In the MD for such reactions the role of the doubly magic lead region ($Z \approx 82$, $N \approx 126$) has been clearly observed. However, the interpretation of such MD is ambiguous. For example, the authors of Refs. [20,21], studying the $^{40}\text{Ar} + ^{238}\text{U}$ reactions, came to the conclusion that the “lead peak” appeared due to the “washing out” of events in the mass region $M_{\text{H}} = 215-230$ as a result of sequential fission. However, the authors of Ref. [22], having studied the $^{40}\text{Ar} + ^{232}\text{Th}$ reaction, retain the opinion that it is a direct manifestation of the strong lead shells. Returning to our $^{48}\text{Ca} + ^{168}\text{Er}$ reaction at $E_{\text{CN}}^* = 39.6$ MeV, we may say that the sequential fission of primary fragments of any mass is unlikely, since their fission probabilities are extremely small [26].

Recently, in the $^{48}\text{Ca} + ^{208}\text{Pb}$, ^{238}U , ^{244}Pu , and ^{248}Cm reactions [27–30], we have observed the effect of closed shells on the properties of quasi-fission at $E_{\text{CN}}^* \approx 30$ MeV. It was found that the shell structure of heavy fission fragments (in the vicinity of ^{208}Pb) as well as of the light ones (in the vicinity of ^{78}Ni) played a role. It is interesting to note that for $^{48}\text{Ca} + ^{208}\text{Pb}$ the main decay channel is classic symmetric fission, and the QF process manifests itself in the form of asymmetric “shoulders,” whose relative yield is much lower [28,29] than found here. We relate this to the fact that in the fission of $^{256}\text{No}^*$, only the light fragments in the quasi-fission shoulders are in the vicinity of magic numbers.

The question arises—why do shell effects in the case of the same nucleus ($^{216}\text{Ra}^*$ here) manifest themselves strongly in the QF process but only weakly in the FF process? This seems to be explained qualitatively by the concept of a di-nuclear system (DNS) [24] (originally elaborated for deep inelastic reactions and then applied to quasi-fission) or by using a “hybrid” model [25] based on a two-center concept. In these models the potential energy plays an important role and depends on the fragment masses formed in the QF process. The potential energy surface (PES) of a DNS is strongly modulated by shell effects. The minima of the PES lie near the doubly magic numbers that play an important role in fission. The DNS excitation energy is counted from the valley in the potential energy surface for each particular mass partition instead of from the ground state of the compound nucleus. Since this is usually slightly higher than the ground state of the CN, the excitation energy of the separate fission fragments is on average lower. Thus, in these models, for the same initial conditions, the QF process is “colder” than normal fission, and the sensitivity to the shell structure is, therefore, higher.

In a recent study of fusion in the systems $^{12}\text{C} + ^{204}\text{Pb}$, $^{19}\text{F} + ^{197}\text{Au}$, and $^{30}\text{Si} + ^{186}\text{W}$ [31], leading to the same compound nucleus that is the object of the present work, an unexpected inhibition of fusion, along with the presence of a significant QF component, was convincingly demonstrated for the two more symmetric systems. However,

this shell effect was not presented in the data of that work [31] (fission-fragment mass distributions are shown for a CN excitation energy of 60 MeV for the three reactions). So shell effects could be significantly suppressed at an excitation energy 20 MeV higher than in this paper. Furthermore, it follows from Ref. [22], as could be intuitively supposed, that the QF contribution to the capture cross section depends strongly on the entrance channel asymmetry. So for lighter projectiles, such as ^{19}F and ^{30}Si , one should expect a smaller effect of QF. A high yield of the QF component in the $^{48}\text{Ca} + ^{168}\text{Er}$ reaction (with even higher entrance-channel symmetry), could suggest that a considerable fusion suppression might be observed in this case as well. In fact we have already performed complementary measurements of fusion-evaporation residues for our two reactions at a number of energies, and the data analysis is in progress.

In conclusion, we have studied mass-energy distributions of fission fragments for two projectile-target combinations— $^{12}\text{C} + ^{204}\text{Pb}$ and $^{48}\text{Ca} + ^{168}\text{Er}$ —that lead to the same compound nucleus $^{216}\text{Ra}^*$ at an excitation energy of around 40 MeV. We have found that the contribution from asymmetric fission in the former reaction is $\approx 1.5\%$, whereas it is $\approx 30\%$ in the latter case. We interpret this dramatic increase in the asymmetric yield as a manifestation of the QF process. In the fission fragment MED for the reaction with ^{48}Ca , shell effects are clearly seen. We interpret the MED for quasifission fragments in a manner analogous to the low-energy fission of heavy nuclei, that is, as a manifestation of an independent decay mode that competes with the normal fusion-fission process. We propose a qualitative explanation of this phenomenon in terms of the concept of a di-nuclear system that never passes through a full CN phase. The greater symmetry of the entrance channel will clearly facilitate the evolution toward the favored QF mass partition, though the higher angular momentum may also play some role.

This work was supported by the Russian Foundation for Basic Research (Grant No. 99-02-17891) and by INTAS (Grant No. 00-655).

-
- [1] M.G. Itkis, V.N. Okolovich, A.Ya. Rusanov, and G.N. Smirenkin, *Fiz. Elem. Chastits At. Yadra* **19**, 701 (1988) [*Sov. J. Part. Nucl.* **19**, 301 (1988)]; *Nucl. Phys.* **A502**, 243 (1989)
 - [2] E.K. Hulet *et al.*, *Phys. Rev. Lett.* **56**, 313 (1986); *Phys. Rev. C* **40**, 770 (1989).
 - [3] U. Brosa, S. Grossmann, and A. Müller, *Phys. Rep.* **197**, 167 (1990).
 - [4] F.-J. Hambsch, F. Vives, P. Sieglar, and S. Oberstedt, *Nucl. Phys.* **A679**, 3 (2000).
 - [5] I.V. Pokrovsky, L. Calabretta, M.G. Itkis, N.A. Kondratiev, E.M. Kozulin, C. Maiolino, E.V. Prokhorova, A.Ya. Rusanov, and S.P. Tretyakova, *Phys. Rev. C* **60**, 041304(R) (1999).
 - [6] M.G. Itkis *et al.*, in *Proceedings of the Tours Symposium on Nuclear Physics III, Tours, 1997*, edited by M. Arnould *et al.*, AIP Conf. Proc. No. 425 (AIP, New York, 1998), p. 189.
 - [7] I.V. Pokrovsky *et al.*, *Phys. Rev. C* **62**, 014615 (2000); G.G. Chubarian *et al.*, *Phys. Rev. Lett.* **87**, 052701 (2001).
 - [8] G. Audi and A.H. Wapstra, *Nucl. Phys.* **A595**, 409 (1995).
 - [9] M.G. Itkis, N.A. Kondratiev, E.M. Kozulin, Yu.Ts. Oganessian, I.V. Pokrovsky, E.V. Prokhorova, and A.Ya. Rusanov, *Phys. Rev. C* **59**, 3172 (1999).
 - [10] J. Töke *et al.*, *Nucl. Phys.* **A440**, 327 (1985); W.O. Shen *et al.*, *Phys. Rev. C* **36**, 115 (1987).
 - [11] J.R. Nix and W.J. Swiatecki, *Nucl. Phys.* **71**, 1 (1965); J.R. Nix, *Nucl. Phys.* **A130**, 241 (1969).
 - [12] G.D. Adeev, I.I. Gonchar, V.V. Pashkevich, N.I. Pischasov, and O.I. Serdyuk, *Fiz. Elem. Chastits At. Yadra* **19**, 1229 (1988) [*Sov. J. Part. Nucl.* **19**, 529 (1988)]; G.D. Adeev and V.V. Pashkevich, *Nucl. Phys.* **A502**, 405 (1989).
 - [13] K.-H. Schmidt *et al.*, *Nucl. Phys.* **A665**, 221 (2000).
 - [14] M.G. Itkis and A.Ya. Rusanov, *Fiz. Elem. Chastits At. Yadra* **29**, 389 (1998) [*Phys. Part. Nucl.* **29**, 160 (1998)].

- [15] R. Bass, Phys. Rev. Lett. **39**, 265 (1977).
- [16] A.V. Ignatuk and I.N. Mikhailov, Communication of JINR, P4-12399, Dubna, 1979.
- [17] M.A. Butler, S.S. Datta, R.T. de Souza, J.R. Huizenga, W.U. Schröder, J. Töke, and J.L. Wile, Phys. Rev. C **34**, 2016 (1986).
- [18] B.B. Back, P.B. Fernandez, B.G. Glagola, D. Henderson, S. Kaufman, J.G. Keller, S.J. Sanders, F. Videbaek, T.F. Wang, and B.D. Wilkins, Phys. Rev. C **53**, 1734 (1996).
- [19] R. Kalpakchieva, Yu.Ts. Oganessian, Yu.E. Penionzhkevich, and H. Sodan, Z. Phys. A **283**, 253 (1977).
- [20] G. Guarino, A. Gobbi, K.D. Hildenbrand, W.F.J. Müller, A. Olmi, H. Sann, S. Bjørnholm, and G. Rudolf, Nucl. Phys. **A424**, 157 (1984).
- [21] G.J. Mathews, L.G. Sobotka, G.J. Wozniak, R. Regimbart, R.P. Schmitt, G.U. Rattazzi, and L.G. Moretto, Z. Phys. A **290**, 407 (1979).
- [22] P. Gippner, K.D. Schilling, W. Seidel, F. Stary, E. Will, H. Sodan, S.M. Lukyanov, V.S. Salamatina, Yu.E. Penionzhkevich, G.G. Chubarian, and R. Schmidt, Z. Phys. A **325**, 335 (1986).
- [23] P. Gippner, U. Brosa, H. Feldmeier, and R. Schmidt, Phys. Lett. B **252**, 198 (1990).
- [24] A. Diaz-Torres, G.G. Adamian, N.V. Antonenko, and W. Seidel, Nucl. Phys. **A679**, 410 (2001); Phys. Rev. C **64**, 024604 (2001).
- [25] V.I. Zagrebaev, Phys. Rev. C **64**, 034606 (2001).
- [26] A.V. Ignatyuk, G.N. Smirenkin, M.G. Itkis, S.I. Mulgin, and V.N. Okolovich, Fiz. Elem. Chastits At. Yadra **16**, 709 (1985) [Sov. J. Part. Nucl. **16**, 307 (1985)].
- [27] M.G. Itkis *et al.*, Nuovo Cimento A **111**, 783 (1998).
- [28] M.G. Itkis *et al.*, in *Proceedings of the 7th International Conference on Clustering Aspects of Nuclear Structure and Dynamics, Rab Island, 1999*, edited by J. Korolija *et al.* (World Scientific, Singapore, 2000), p. 368.
- [29] M.G. Itkis *et al.*, in *Proceedings of the International Conference on Fission and Properties of Neutron-Rich Nuclei, St. Andrews, 1999*, edited by J.H. Hamilton *et al.* (World Scientific, Singapore, 2000), p. 268.
- [30] M.G. Itkis *et al.*, in *Proceedings of the International Conference on Nuclear Physics at Border Lines, Lipari (Messina), 2001*, edited by G. Fazio *et al.* (World Scientific, Singapore, 2002), p. 146.
- [31] A.C. Berriman *et al.*, Nature (London) **413**, 144 (2001); in *Proceedings of the International Nuclear Physics Conference, INPC 2001, Berkeley, 2001*, edited by E. Norman *et al.*, AIP Conf. Proc. No. 610 (AIP, New York, 2002), p. 608.